# Gas visualization of industrial hydrocarbon emissions

Sandsten, Jonas; Edner, Hans; Svanberg, Sune

*Published in:*
Optics Express

2004

# Gas visualization of industrial hydrocarbon emissions

**Jonas Sandsten*, Hans Edner* and Sune Svanberg**
*Department of Physics, Lund Institute of Technology,*
*P.O. Box 118, S-221 00 Lund, Sweden,*

**Present address: GasOptics Sweden AB, Ideon Science Park,*
*Ole Römers väg 16, S-223 70 Lund, Sweden*
jonas.sandsten@gasoptics.com

**Abstract:** Gases leaking from a polyethene plant and a cracker plant were visualized with the gas-correlation imaging technique. Ethene escaping from flares due to incomplete or erratic combustion was monitored. A leakage at a high-pressure reactor tank could be found and visualized by scanning the camera system over the industrial site. The image processing methods rely on the information from three simultaneously captured images. A direct and a gas-filtered infrared image are recorded with a split-mirror telescope through a joint band-pass filter. The resulting path-integrated gas concentration image, derived from the two infrared images, is combined with a visible image of the scene. The gas-correlation technique also has the potential to estimate the flux in the gas plume by combining a wind vector map, derived by cross-correlating the images in time, with a calibrated gas path-integrated concentration image. The principles of the technique are outlined and its potential discussed.



**OCIS codes:** (040.3060) Infrared; (110.3080) Infrared imaging; (280.1120) Air pollution monitoring; (300.6340) Spectroscopy, infrared.

## References and links

1. J. Sandsten, H. Edner, and S. Svanberg, "Gas imaging by infrared gas-correlation spectrometry," Opt. Lett. **21**, 1945 (1996).
2. J. Sandsten, P. Weibring, H. Edner, and S. Svanberg, "Real-time gas-correlation imaging employing thermal background radiation," Opt. Express **6**, 92 (2000); http://www.opticsexpress.org/abstract.cfm?URI=OPEX-6-4-92
3. P. Weibring, H. Edner, and S. Svanberg, "Versatile mobile lidar system for environmental monitoring," Appl. Opt. **42**, 3583 (2003).
4. H. Edner, S. Svanberg, L. Unéus, and W. Wendt, "Gas-correlation lidar," Opt. Lett. **9**, 493 (1984).
5. T. J. Kulp, P Powers, R. Kennedy, and U-B. Goers, "Development of a pulsed backscatter-absorption gas-imaging system and its application to the visualization of natural gas leaks," Appl. Opt. **37**, 3912 (1998).
6. P. Weibring, M. Andersson, H. Edner, and S. Svanberg, "Remote monitoring of industrial emissions by combination of lidar and plume velocity measurements," Appl. Phys B **66**, 383 (1998).
7. P. E. Powers, T. J. Kulp, and R. Kennedy, "Demonstration of differential backscatter absorption gas imaging," Appl. Opt. **39**, 1440 (2000).
8. J. Sandsten, "Development of infrared spectroscopy techniques for environmental monitoring," Lund Reports on Atomic Physics **LRAP-257**, 2000.
9. OSLO, Optics Software for Layout and Optimization, Ver 5.4, Sinclair Optics 2000.
10. P. S. Andersson, S. Montán, and S. Svanberg, "Multi-spectral system for medical fluorescence imaging," IEEE J. Quantum Electron. **QE-23**, 1798 (1987).
11. Camera system specifications; Detector: MCT Sprite Stirling, 4–13 µm, NE$\Delta$T = 80 mK, Filterwheel with 5 positions; Visualised gases: Methane, Ethene, Ammonia, Nitrous Oxide; Ammonia: Detection limit 30 ppm × m at $\Delta$T = 18 K with split-image telescope (present), Range and resolution: 10-1000 meters, 136 × 136 pixels gas image combined with high resolution visible image; Frame rate: 15 images/s.

#3883 - $15.00 US Received 25 February 2004; revised 18 March 2004; accepted 30 March 2004

## 1. Introduction

Visualization of gases from industrial areas is of interest for many reasons. Hydrocarbon gas emissions are important for environmental considerations. Health and safety of the operating personnel at petrochemical plants are directly affected by gas emissions at the workplace. Monitoring of gas leaks is therefore of great importance in controlling and stopping gas outflow. Easily deployable surveillance techniques for assessing sites of accidents involving gas tankers or trains are desirable for safety considerations.

We have developed a technique for the imaging of a certain gas employing IR cameras and gas filter correlation techniques [1]. Our first measurements were performed using a camera sensitive in the 3-5 μm region. More recently, a camera sensitive in the 8-12 μm region and a split-mirror Cassegrainian telescope has been employed, enabling passive gas imaging through absorption or emission of thermal radiation [2]. The present paper illustrates gas visualization and leak detection at a polyethene producing petrochemical plant in Sweden. Specific gas visualization and quantification with a technique that relies on passive background radiation and elimination of problems with interfering gases, aerosol particles and varying background radiation have not existed until now. Two complementary techniques, based on lasers are the LIDAR (light detection and ranging) and the BAGI (backscatter absorption gas imaging) techniques [3-5]. The lidar technique has been used to map cross-sections of the air downwind from industrial sites by vertical scanning a pulsed laser beam [6]. The lidar systems are based on sensitive and costly laser systems often placed in trucks on optical tables. The lidar technique is especially interesting for environmental protection authorities because of the possibility to ascribe a total flux to an industrial site of diffuse leaks. The bagi technique is based on a laser, which is spectrally tuned to a gas absorption line and synchronously scanned with an infrared sensitive camera. The method depends on diffusely backscattered light from a surface with an even reflectance behind the gas and the speckle noise in the images produced is of concern. Some improvements of the image quality can be made by using a differential technique with two wavelengths [7]. The use of a high-power laser makes eye safety a problem when searching for real leaks in an industrial site. Both the lidar and the bagi techniques depend on lasers and are therefore not as flexible and viable as the new gas-correlation imaging technique. The requirements on explosion-proof equipment in hazardous areas are also more difficult to meet with laser-based techniques.

## 2. Measurements

Performing gas visualization at industrial sites places a number of demands on the monitoring system. The most important system characteristics, some of them may seem obvious, are a rugged and compact design, an easily moveable setup and insensitivity to interference, such as from varying background emissivities and other gases including the frequently occurring water vapor. The precise location of a leak must also be registered in parallel with the detection of emitted gas. The gas of interest must be visualized at least at concentration levels prescribed by the regulating authorities. As an example, in the Swedish oil industry the operating personnel will immediately fit tight a hydrocarbon leak if its value is above 900 ppm (measured as a propane equivalent with a calibrated point monitoring instrument as close to the potential leak as possible). A leak between 100-900 ppm should be taken care of on a scheduled basis, and leaks below 100 ppm can be left without taking any measures. Finally, the measurements must not disturb the activities in the industrial site.

The detection system that solves the problems mentioned above is based on the passive two-dimensional gas-correlation principle. It consists of a newly developed split-mirror telescope, an infrared camera and a ccd camera used for taking visible images. The essential component in optical and spectroscopic gas correlation is the split-mirror telescope [8]. The telescope was designed and evaluated using a ray-tracing program [9] and it has enhanced the signal-to-noise ratio and improved the image quality of the real-time gas correlation movies compared to a former solution, which was based on a Cassegrainian telescope [10]. It takes less than 10 minutes to set the system up and start taking the first gas images. The distance to

#3883 - $15.00 US Received 25 February 2004; revised 18 March 2004; accepted 30 March 2004

the objects is normally between 10 and 1000 meters. The infrared camera generates an image built up from 272 x 136 pixels making it well suited for the formation of two 136 x 136 pixels images at the same time [11]. Visible images are generated together with the gas images and used as a background to guide the eye and locate the leakage. The camera system made it possible for us to visualize ethene gas clouds and leakages from a polyethene plant and a cracker plant in Sweden. The system is shown in Fig. 1 in front of the cracker plant.

Fig. 1. The gas-correlation infrared camera system in front of a cracker plant.

The measurement positions could be chosen freely inside the site or outside the fence. A major feature of the passive gas-correlation imaging is the possibility to visualize and measure gas emissions from places difficult to access with other methods. A flare is exceedingly hard to monitor but an important contributor of hydrocarbons if the combustion is incomplete or erratic. The combustion of ethene should preferably always be visualized and optimized in the flare. During the flare measurements at the petrochemical plant the meteorological conditions were: varying wind speeds (mean value 4 m/s) and directions, air temperature 5 °C and the blue sky or clouds were providing the background. The detection limit of the passive gas-correlation method is strongly influenced by the temperature difference between the gas cloud of interest and the background [2]. We make the assumption that the ethene gas temperature quickly assumes the same temperature as the surrounding air. The gas reaches thermal equilibrium with the air downwind the flare exit, through vibrational and rotational relaxation during mixing with the air molecules, in a few seconds. It should be noted, that it is necessary to measure sufficiently far downwind from an optically thick outlet, so that the plume becomes optically thin; in order to derive the concentration times length (path-integrated concentration) through the plume for flux evaluations. This is in practice tens of meters from the flare exit. A projected wind vector is derived by cross-correlating the processed gas-correlation images in time. The image processing will be described in detail in Section 4.

### 3. Results

Flares are used to burn excess hydrocarbon gases, hydrogen and other gases. By directing the camera system to flares, we could visualize the flow of ethene that escapes from the flares.

#3883 - $15.00 US Received 25 February 2004; revised 18 March 2004; accepted 30 March 2004

Two flares at the polyethene plant, LT1 and LT2, have a height of 40 m and in our measurements they were 340 m and 430 m from the camera system, respectively. A photograph of the flare LT1 is shown in Fig. 2(a). The result from the LT1 flare, after gas-correlation image processing and merging with a visible ccd image, is shown in Fig. 2(b) as a movie. We could observe water vapor just above the exits with the naked eye and the ccd camera, as shown in Fig. 2(b).

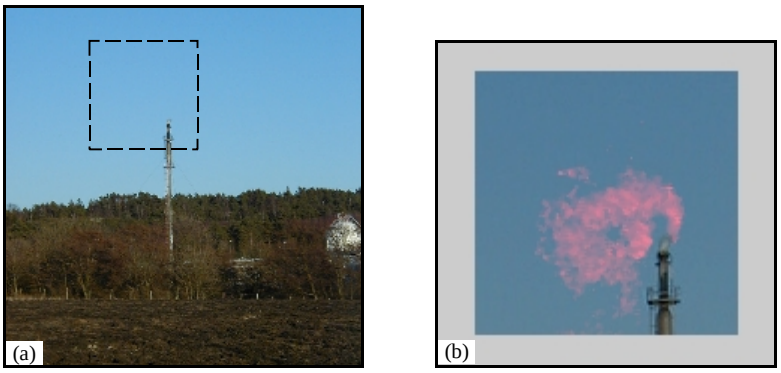


Fig. 2. (a) Flare LT1 at the polyethene plant. (b) (2.0 MB) Movie of ethene gas cloud escaping from flare LT1 as visualized with the system (6.0 MB version).

Thirty minutes after the image in Fig. 2. was captured, the high pressure (2300 bar) reactor tank safety valve released 1 – 2 tons of ethene in five minutes to the atmosphere. The gas cloud covered the industrial site for 15 minutes before it was blown away and diluted in air. A visible ccd image of the site is shown in Fig. 3.

Fig. 3. Image of the polyethene plant taken from the same position as the flare measurements. The high pressure reactor is seen behind the gas purification site in the middle of the image.

The ethene gas cloud is visualized in three scenes in Fig. 4 and Fig. 5. These recordings were taken with a simpler detection system, employing an infrared camera based on a staring microbolometer detector. According to the environmental officer, these events occur once or twice a month. Being able to monitor events of large emissions occurring in a very short time could improve total flux estimates significantly. Spike-like emissions are often discriminated from regular monitoring measurements and labeled outliers, but the inclusion of such events is of great importance for controlling authorities. Visualizing such events has the strong pedagogical power of images and pinpoints environmental problems.

#3883 - $15.00 US Received 25 February 2004; revised 18 March 2004; accepted 30 March 2004

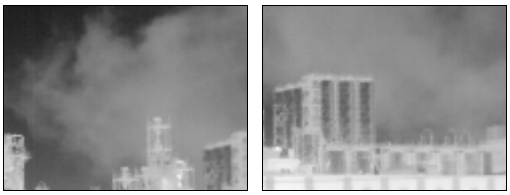

Fig. 4. Optically dense ethene gas cloud one minute after the safety valve release.

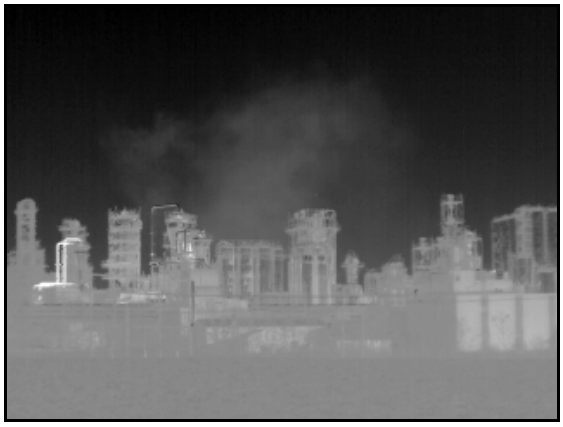

Fig. 5. Ethene gas cloud covering part of the industry five minutes after the high-pressure reactor safety valve release of 1 – 2 tons of ethene into the atmosphere.

So far, all the measurements were performed from outside the plant during the evening before the official measurement day. The next day we started measurements at the gas purification site and monitored the flares again. During that sample test, the flares did not burn any ethene or they were not fed with ethene. By sweeping the camera system over the polyethene plant, we could find an ethene leakage despite the presence of the interference from water vapor and other gases. This leak was taken care of immediately by the operating personnel. The leak was due to a sheaving valve in connection with the high-pressure reactor gas release the evening before. This leak is visualized in Fig. 6.

Fig. 6. (1.6 MB) Movie of ethene leakage. By sweeping the camera system over the polyethene plant, a leakage was found. A visible image and a sequence of gas images are shown. The gas-correlated images are merged with the zoomed visible image. The ethene gas leakage was taken care of immediately by the operating personnel (3.8 MB version).

#3883 - $15.00 US Received 25 February 2004; revised 18 March 2004; accepted 30 March 2004

Measurements were also performed on the cracker plant flares with the camera system placed outside the fence at the power-interlocking machine. It was not clear, by the beforehand information from the environmental officer, whether the flares were burning ethene during the sample test, or some other gas, but the result clearly showed that no ethene escaped from the flares. This indicates that no ethene was fed to the flares. Otherwise, there would have been traces of ethene gas. At the next site, in close proximity to a small oil harbor, we used the camera system in both the absorption and the emission modes of operation. Flares were monitored in emission against clouds in the background sky and the hot cracker plant was used as the background in the gas absorption mode.

Searching for leaks and fitting them tight is of interest from an economical point of view, because it can reduce valuable raw material spill, but it is also extremely valuable for the operating personnel, because of health and safety aspects. Further, the awakening environmental consciousness among the public cannot allow greenhouse gas emissions that could easily be visualized and eliminated.

## 4. Gas-correlation telescope design and image processing

In this section, we will describe the gas-correlation image processing in detail. The final images in the previous section will be dealt with and the derivation of the path-integrated concentration, the procedures for retrieving the wind vector and the flux calculations will be explained. Two image-processing strategies have been developed and they are selected depending on how we want to visualize the flowing gases. The first strategy is used when searching for leaks and the other one is used if there is a need for flux measurements. The reasons for dividing the image processing into two parts are that searching for specific gas leaks can be made in real-time, while the flux measurements involve cross-correlation of complete matrixes, which is time consuming and therefore is better suited for post processing. The image generating system including the new design of the split-mirror telescope will also be evaluated and compared with the former system.

In earlier work on gas visualization, we have been using a Cassegrainian telescope designed for a completely different application [9]. The telescope consists of a primary spherical mirror divided into four separated parts and a secondary spherical mirror. This telescope is a classical Cassegrainian design except for the possibility to fine adjust the positions of four images. The design was found to cause a number of image errors, which are described in Ref. [7]. Here we will summarize the results from ray-tracing [8] of the Cassegrainian telescope and compare the design with the results from ray-tracing of the new Gas-Correlation Telescope (GCT), see Table 1.

Table 1. Comparison of the two telescopes used for gas-correlation imaging.

| | **Cassegrainian Telescope** | **Gas-Correlation Telescope** |
|---|---|---|
| Primary mirror | Spherical | Off-axis parabolic |
| Secondary mirror | Spherical | Folded planar |
| Focal length (mm) | 194 | 305 |
| Reduction | 1:1550 | 1:980 |
| Opening diameters (mm) | 43 | 43 |
| **Ray-tracing results:** | | |
| Spherical abberation coeff. | -1.84 | 0.006457 |
| Spot size radius on axis (μm) | 100 | 22 |

The Cassegrainian telescope is based on two spherical mirrors, which are used off-axis. The spherical abberation coefficient is therefore the largest abberation representing the transverse displacement in the paraxial image plane. With the new gas-correlation telescope design, a diffraction limited spot size radius five times smaller than the former Cassegrainian design

#3883 - $15.00 US Received 25 February 2004; revised 18 March 2004; accepted 30 March 2004

was reached. This was accomplished by using off-axis parabolic mirrors and planar mirrors for motorized focusing and ray folding. A ray-trace of the GCT with an object of five meters height, placed 300 meters from the telescope results in the rays shown in Fig. 7, forming two simultaneous images of 5.1 mm height each.

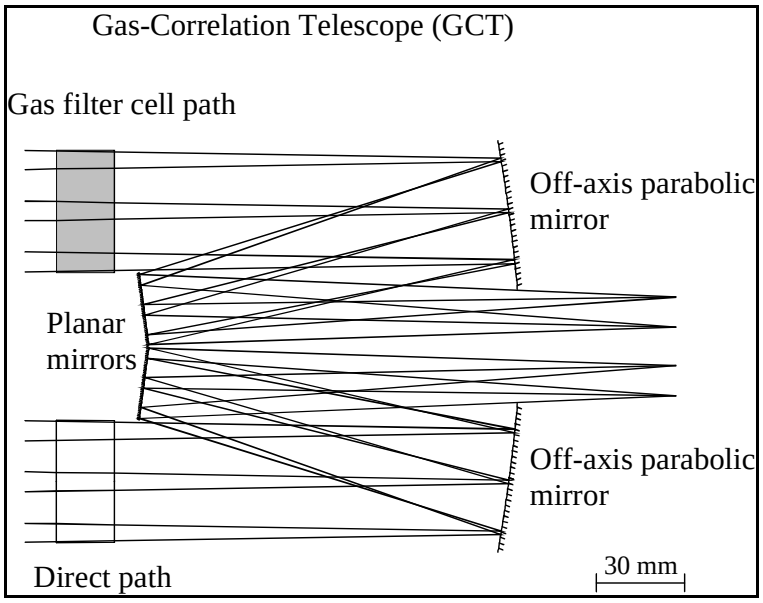


Fig. 7. Ray-tracing the gas-correlation telescope.

The new telescope design enabled us to find specific gas leaks in the industrial environment as reported in the results section before. The raw images belonging to the result image in Fig. 2, of the flare at LT1, are shown in Fig. 8. Both images are captured at the same time with the infrared camera [11] equipped with a bandpass filter; the left image in the figure is a direct infrared image of the flare and all the gases and water vapor that are escaping. The right image in Fig. 8 is an ethene gas-filtered image, showing the same objects as in the direct infrared image but no ethene. Notice the self-emission from the ethene in the gas cell, seen all over the image as a minor brightness increase.

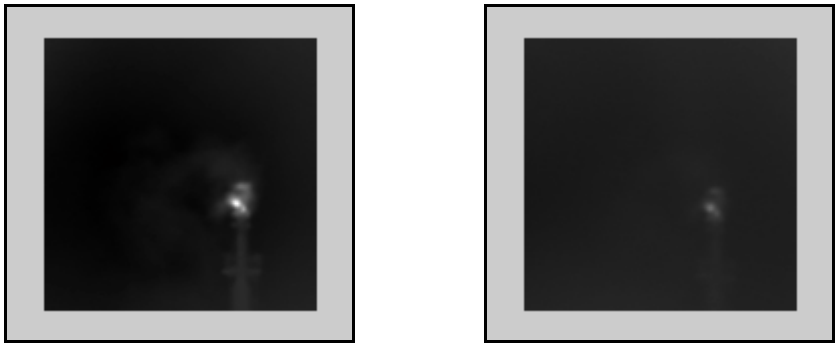

Fig. 8. Raw split-mirror image of the flare at LT1. The left part of the figure shows the infrared image of the flare and at the same time the ethene gas-filtered image is captured and shown to the right in the figure.

From the raw images, we subtract a background image that includes telescope and gas cell self-emission. This image is recorded against the sky background. The result is shown in Fig. 9. The next step in the image processing is to divide the infrared image with the ethene gas-

#3883 - $15.00 US Received 25 February 2004; revised 18 March 2004; accepted 30 March 2004

filtered image. After that step we reduce the salt-and-pepper noise with median filtering and enhance the contrast by thresholding the image with respect to a residue of ethene that survives the division. The resulting ethene gas images are then merged with visible images and presented as a movie, Fig. 2(b).

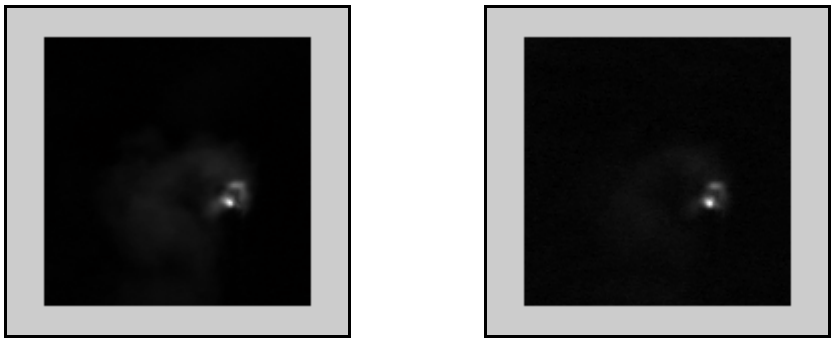

Fig. 9. Raw split-mirror image of the flare at LT1 with the background image removed.

The leak image as shown in Fig. 6 that was obtained as part of a sweep of the camera system field of view over the polyethene plant, was processed as the flare, except for a stronger thresholding, that yielded binary images. The gas is coded as one where it is detected and zero everywhere else in the gas image.

With a calibrated gas-correlated image as discussed in Ref. [2], the flux can be calculated using techniques described in Ref. [6]. The path-integrated concentration in Fig. 10(a) corresponding to the individual pixel values are summed in the column depicted by the vertical bar, shown in Fig. 10(b). The wind is blowing from the right in the image and downwind at the vertical bar, the gas cloud is optically thin.

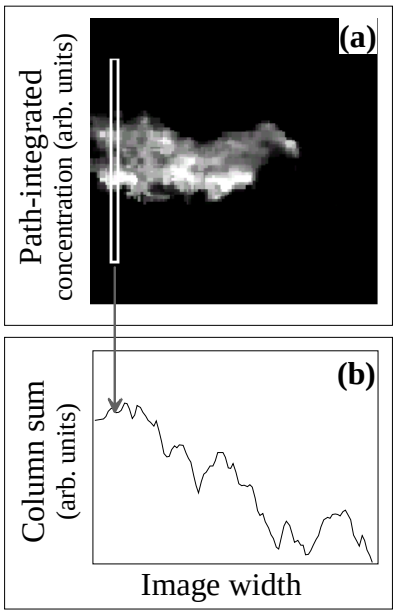


Fig. 10. (a) Gas-correlated ethene image. The concentration times the depth in the image corresponds to a pixel value in the calibrated image. (b) By summing the pixel values in the column downwind where the gas cloud is optically thin, depicted by the vertical bar, and multiplying the sum with the wind vector obtained from cross-correlating two gas images in time, the ethene flux can be estimated.

#3883 - $15.00 US Received 25 February 2004; revised 18 March 2004; accepted 30 March 2004

A wind vector map is derived by cross-correlating a small matrix in an image at time $T_0$ (Fig. 11(a)) with a corresponding small matrix in an image at a later time, $T_1$ (Fig. 11(b)). The size of the small matrixes are chosen by maximizing the cross-correlation product. By creating and moving the cross-correlation matrixes over the complete images a resulting time-correlated wind vector map can be produced. The resulting wind vector map merged with the image at time $T_0$ is shown in Fig. 11(c). A typical time interval, $T_1$-$T_0$, has been 1/15 s.

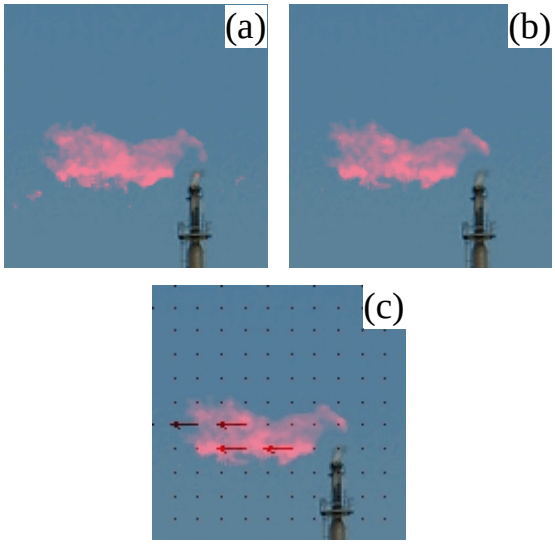


Fig. 11. (a) Gas-correlated ethene image at time $T_0$. (b) Gas-correlated ethene image at time $T_1$. (c) Wind vector map derived by cross-correlating the gas-correlated images at time $T_0$ and $T_1$. The resolution of the vector map is determined by the size of the small cross-correlation matrixes.

The magnitude of the wind vectors in Fig. 11(c) are varying from 6.6 m/s to 7.1 m/s. The leftmost arrow in Fig. 11(c) multiplied with an ethene calibrated pixel value in Fig 10(a) would yield the flux of ethene from the flare.

## 5. Discussion

We have showed that the gas-correlation imaging technique is well suited for industrial leakage detection and visualization. The imaging methods described can also be used for flux determinations. Incomplete flare combustion can be monitored in real-time using the emission mode. The main advantage of the passive gas-correlation method is the simultaneous capture of two images, which are divided, yielding a result image free from interfering gases and varying background conditions. A great advantage over active methods is that there is no need for a costly and sensitive laser or spectrometer. The gas-correlation cell acts as a perfectly matched specific gas filter.

Further improvments of the gas-correlation technology include the development of a methane gas visualization system within the spin-off company GasOptics Sweden AB. The system will be used to detect, visualize and localize methane leaking from gas processing plants. The distance from the camera system to the petrochemical plant can be chosen between 10-1000 m. Future prospects include the calibration of several hydrocarbon gases as described in Ref. [2] and adaptation of the technique to other applications.

## Acknowledgments

This work was supported by the Knut and Alice Wallenberg Foundation.

#3883 - $15.00 US Received 25 February 2004; revised 18 March 2004; accepted 30 March 2004